Efficient Velocity-Based Quasi-Linear Model Predictive Control for Wind Turbine Side-Side Tower Periodic Load Reductions

de Neves de Fonseca, M.; Pamososuryo, Atindriyo K.; Mulders, Sebastiaan P.

DOI
10.1109/LCSYS.2024.3508616

Publication date
2024

Document Version
Final published version

Published in
IEEE Control Systems Letters

Efficient Velocity-Based Quasi-Linear Model Predictive Control for Wind Turbine Side-Side Tower Periodic Load Reductions

Maria de Fonseca, Atindriyo K. Pamososuryo, and Sebastiaan P. Mulders, *Member, IEEE*

***Abstract*—Advancements in wind turbine technology have made wind energy more cost-competitive. While taller towers use less material, they are more susceptible to fatigue. This letter introduces a convex model predictive control scheme to actively counteract side-side periodic loads using a velocity-based approach, which captures the system's nonlinear behavior without requiring extensive prior operating points. A quasi-linear parameter-varying dynamic model for wind turbine towers is established through model demodulation transformation. Simulation results show a 96% reduction in net force in the side-side direction at the tower top under turbulent wind conditions.**

***Index Terms*—Energy systems, linear parameter-varying systems, predictive control for nonlinear systems.**

I. Introduction

RECENT advancements in wind energy, particularly the increase in size and power capacities of wind turbines, have significantly improved its cost-competitiveness. Taller towers and larger rotors enable wind turbines to tap into superior wind resources at higher altitudes and capture more power, driving down overall costs [1]. However, the realization of such taller towers necessitates a reduction in material usage [2], which makes the towers more susceptible to side-side periodic loads and resonant behavior due to the resulting flexibility, leading to accelerated material degradation. Rotor mass and aerodynamic imbalances, either inherent in the manufacturing process or developed over time, give rise to these susceptibilities. Research has been done to estimate these imbalances [3], as safe operations of wind turbines require well-balanced rotors.

Conventionally, to actively control turbine side-side tower motion induced by wind excitations, either generator torque [4], [5] or individual blade pitching [6], [7] can be used. Generator torque affects power quality as it is directly coupled with power generation, while individual pitch increases the wear and tear of the pitch mechanism. A more passive method aiming to prevent prolonged resonance excitation—in the literature referred to as 'frequency-skipping' by imposing speed exclusion zones—can be helpful when the rotational frequency (1P) or blade passing frequency (3P, for a three-bladed turbine) excites a structural resonance at a particular operating point [8]. As a result, the rotor speed passes through the critical speed range without severely exciting the natural frequency by modifying the speed-torque curve [9], [10]. However, such methods may not be able to systematically balance objectives nor take into account system constraints. To address this issue, advanced control strategies such as Model Predictive Control (MPC) have been proposed as they take in constraints and objectives.

The current advanced predictive methods for mitigating tower side-side periodic loads are mainly focused on passive, frequency-skipping approaches. For instance, [11] takes advantage of a quasi-Linear Parameter-Varying (quasi-LPV) model of the wind turbine derived through the use of Model Demodulation Transformation (MDT) techniques followed by Jacobian linearization to obtain a convex optimization problem. The model is then controlled by a quasi-Linear MPC (qLMPC) controller. While this effectively prevents extended operation at critical rotational speeds, it lacks the ability to actively alleviate periodic loads as the periodic side-side loading is often unknown in practical situations. To address this limitation, [12] introduces a Kalman filter for online estimation of the periodic loading.

The work in [13] explores a velocity-based linearization approach for obtaining a quasi-LPV model of the wind turbine dominant dynamics for fore-aft damping control using a velocity-based qLMPC scheme. The advantage of velocity-based compared to Jacobian linearization is the elimination of the need to store equilibrium input and state vectors.

This letter proposes an active control scheme for mitigating side-side periodic disturbances by combining MDT and velocity-based techniques into a computationally efficient qLMPC algorithm. The two main contributions are:

1) integrating MDT techniques with velocity-based linearization to create a unified quasi-LPV model of the wind turbine tower and aerodynamics;
2) designing a velocity-based qLMPC scheme to actively cancel periodic loads targeting side-side motion.

The developed framework offers significant technological advantages and operates online. It eliminates the need to store operating points, unlike in [11], and is less demanding than nonlinear control techniques like nonlinear MPC, which can be complex for real-time applications [14]. Additionally, it accounts for physical and saturation constraints, allows intuitive calibration of the cost function through weight

Received 28 August 2024; revised 30 October 2024; accepted 16 November 2024. Date of publication 27 November 2024; date of current version 6 December 2024. Recommended by Senior Editor S. Olaru. *(Corresponding author: Maria de Fonseca.)*

The authors are with the Delft Center for Systems and Control, Delft University of Technology, 2628 CD Delft, The Netherlands (e-mail: M.deNevesdeFonseca@tudelft.nl; A.K.Pamososuryo@tudelft.nl; S.P.Mulders@tudelft.nl).

Digital Object Identifier 10.1109/LCSYS.2024.3508616

assignment, and yields optimal solutions, contrasting with empirical methods based on fundamental control theory [6].

This letter is organized as follows. Section III introduces LPV systems and their benefits for controlling nonlinear systems affected by unknown external signals, including predictive control through quasi-LPV representation and velocity-based linearization. Section IV summarizes MDT theory. Section V presents the wind turbine aerodynamics and tower demodulated model and proposes a side-side load mitigation framework. Section VI includes simulation results, and Section VII concludes and offers recommendations for future research.

II. Prerequisites and Assumptions

This letter uses a series of assumptions outlined in this section. Although certain assumptions can be eased, this letter primarily emphasizes the fundamental working principles of the implemented control algorithm.

Assumption 1: The turbine is considered to function solely within the partial-load region,[1] controlled by generator torque, and maintaining a constant fine pitch angle.

Assumption 2: The rotor acceleration, the wind speed and the side-side periodic load are assumed to be available and measured deterministic signals.

Assumption 3: Disturbances such as wind speed and side-side periodic load are assumed to be invariant over the optimization prediction horizon at each simulation time step.

Assumption 4: A baseline and optimally calibrated torque controller provides optimal power production performance.

III. Velocity-Based Quasi-Linear Model Predictive Control

A nonlinear system can often be described around an equilibrium by a Linear Time-Invariant (LTI) model through Jacobian linearization. This allows for the use of linear control design techniques, but the model validity is limited to a small region around that equilibrium. When control across a wider range is desired or the system's dynamics depend on an external parameter, a more complex mathematical model framework is necessary. Such a framework is referred to as an LPV model [15], which still presents a linear relationship between the input and output, but this relationship may now depend on exogenous non-stationary parameters:

$$\begin{aligned}\dot{x}(t) &= A(\theta(t))x(t) + B(\theta(t))u(t),\\ y(t) &= C(\theta(t))x(t) + D(\theta(t))u(t),\end{aligned} \tag{1}$$

where $A \in \mathbb{R}^{n_x \times n_x}$, $B \in \mathbb{R}^{n_x \times n_u}$, $C \in \mathbb{R}^{n_y \times n_x}$ and $D \in \mathbb{R}^{n_y \times n_u}$ are continuous maps, $u \in \mathbb{R}^{n_u}$ is the input, $y \in \mathbb{R}^{n_y}$ is the output, $x \in \mathbb{R}^{n_x}$ is the state variable, and $\theta \in \mathbb{R}^{n_\theta}$ is an external parameter that can depend on time [16]. The latter is also referred to as external *scheduling variable*. The parameter vector $\theta(t)$ belongs to a compact set of admissible values, i.e., $\theta(t) \in \Theta \subseteq \mathbb{R}^{n_\theta}\ \forall t \geq 0$ [17]. Hereafter, the time dependence of $\theta(t)$ will be omitted for brevity's sake.

A. Quasi-LPV Systems

When θ is defined as an external signal characterized by unknown and unpredictable future values, it falls under the category of a *general* LPV system. In contrast, when θ is used to model nonlinear dynamics, becoming a function of the system's states and inputs, it is possible to predict its future values. This is known as a *quasi*-LPV system [18].

[1]Region of operation where wind speeds are lower than rated.

A quasi-LPV system meets the LPV system definition outlined in (1), where the time-varying parameters are determined by functions of inherent signals (i.e., states and inputs): $\theta = \vartheta(x(t), u(t))$. Here, $\vartheta : \mathbb{R}^{n_x} \times \mathbb{R}^{n_u} \to \mathbb{R}^{n_\theta}$ is a continuous function on the compact set of admissible values Θ.

B. Conventional qLMPC Algorithm

A recent study has introduced a predictive algorithm known as qLMPC [19] to control quasi-LPV systems summarized here. Consider the following discrete-time state evolution:

$$x_{k+1} = A(\theta_k)x_k + B(\theta_k)u_k, \tag{2}$$

where $u \in \mathbb{R}^{n_u}$ is the input, $x \in \mathbb{R}^{n_x}$ is the state, $\theta_k = \vartheta(x_k, u_k) \in \mathbb{R}^{n_\theta}$ is the scheduling variable, and $\vartheta \in \mathbb{R}^{n_\theta}$, $A \in \mathbb{R}^{n_x \times n_x}$ and $B \in \mathbb{R}^{n_x \times n_u}$ are continuous maps. Let it be assumed that $\theta_k \in \Theta, \forall k \geq 0$. Furthermore, the pair $(A(\theta), B(\theta))$ is stabilizable $\forall \theta \in \Theta$.

The sequence of actions U_k inside the prediction horizon N is defined as the following column vector:

$$U_k = \begin{bmatrix} u_k^\top & u_{k+1}^\top \cdots u_{k+N-1}^\top \end{bmatrix}^\top \in \mathbb{R}^{Nn_u}, \tag{3}$$

which is determined by solving the given problem:

$$\begin{aligned}\min_{U_k}\ & J_k(U_k)\\ \text{s.t.}\ & x_{k+i} = A(\theta_{k+i-1})x_{k+i-1} + B(\theta_{k+i-1})u_{k+i-1},\\ & u_{k+i-1} \in \mathcal{U}, \quad x_{k+i-1} \in \mathcal{X} \quad \forall i \in [1, \ldots, N],\\ & x_{k+N} \in \mathcal{X}_f,\end{aligned} \tag{4}$$

where J_k is the finite horizon cost. It is assumed that $\vartheta(\mathcal{X}_f \times \mathcal{U}) \subset \Theta$ [19]. Moreover, the following are defined:

$$\begin{aligned}X_k &= \begin{bmatrix} x_{k+1}^\top & x_{k+2}^\top \cdots x_{k+N}^\top \end{bmatrix}^\top \in \mathbb{R}^{Nn_x},\\ T_k &= \vartheta\left(\begin{bmatrix} x_k^\top & X_k^\top \end{bmatrix}^\top, U_k\right) = \begin{bmatrix} \theta_k^\top & \theta_{k+1}^\top \cdots \theta_{k+N-1}^\top \end{bmatrix}^\top \in \mathbb{R}^{Nn_\theta},\end{aligned} \tag{5}$$

where X_k is a column vector of states and T_k is the collection of scheduling variables at each time step over the prediction horizon N. Definitions (3) and (5) give the prediction model:

$$X_k = \Lambda(T_k)x_k + S(T_k)U_k, \tag{6}$$

with the matrices $\{\Lambda, S\}$ being

$$\Lambda(T_k) = \begin{bmatrix} A(\theta_k) \\ A(\theta_{k+1})A(\theta_k) \\ \vdots \\ A(\theta_{k+N-1}) \cdots A(\theta_k) \end{bmatrix},$$

$$S(T_k) = \begin{bmatrix} B(\theta_k) & 0 & \cdots \\ A(\theta_{k+1})B(\theta_k) & B(\theta_{k+1}) & \cdots \\ \vdots & \vdots & \ddots \\ A(\theta_{k+N-1}) \cdots A(\theta_{k+1})B(\theta_k) & A(\theta_{k+N-1}) \cdots A(\theta_{k+2})B(\theta_{k+1}) & \cdots \end{bmatrix}.$$

Using this, the cost function $J_k(U_k)$ can be written as

$$\begin{aligned}J_k(U_k) = &(\Lambda(T_k)x_k + S(T_k)U_k)^\top \tilde{Q}(\Lambda(T_k)x_k + S(T_k)U_k)\\ &+ U_k^\top \tilde{R} U_k + V_f(x_{k+N}),\end{aligned} \tag{7}$$

with $\tilde{Q} = \text{diag}_N(Q) \in \mathbb{R}^{N \times N}$ and $\tilde{R} = \text{diag}_N(R) \in \mathbb{R}^{N \times N}$. Note that $Q = Q^\top \succeq 0 \in \mathbb{R}^{n_x \times n_x}$, $R = R^\top \succ 0 \in \mathbb{R}^{n_u \times n_u}$ are weighting matrices penalizing the states and control inputs, respectively. The terminal cost is given as V_f.

At each time step, the scheduling sequence T_k^l is iteratively updated to reach its optimal value $T_k^* = \vartheta(X_k^*, U_k^*)$. In each iteration step l, an optimization problem resembling (4) is solved. The stopping criteria can be defined, for instance, as $|T_k^l - T_k^{l-1}| < \epsilon$, where ϵ is a predefined error threshold. Once this condition is satisfied, the input sequence U_k^l is used

as an approximation of the optimal solution U_k^* to (4). The obtained X_k^l and U_k^l are applied in the subsequent time step $k+1$ to compute $T_{k+1}^0 = \vartheta(X_k^l, U_k^l)$ while the iteration count l is reset to zero. This approach, known as *warm-start*, aids in achieving faster convergence. For more information and pseudo-algorithm the reader is referred to [19].

C. Velocity-Based Linearization Towards a Quasi-LPV Model

Velocity-based linearization of the nominal plant readily provides a quasi-LPV model. Let the following nonlinear system dynamics be given:

$$\dot{x}(t) = f(x(t), u(t)), \quad y(t) = h(x(t), u(t)), \tag{8}$$

where $f(x(t), u(t)) : \mathbb{R}^{n_x \times n_u} \to \mathbb{R}^{n_x}$ and $h(x(t), u(t)) : \mathbb{R}^{n_x \times n_u} \to \mathbb{R}^{n_y}$ are some nonlinear functions that can depend on the input $u \in \mathbb{R}^{n_u}$ and state $x \in \mathbb{R}^{n_x}$, and $y \in \mathbb{R}^{n_y}$ is the output. For simplicity, it is assumed that the output is only influenced by the states. These dynamics can be described by the relationship between the state and input derivatives:

$$\begin{aligned}\ddot{x}(t) &= \underbrace{\nabla_x f(x(t), u(t))}_{A_c(x(t),u(t))} \dot{x}(t) + \underbrace{\nabla_u f(x(t), u(t))}_{B_c(x(t),u(t))} \dot{u}(t),\\ \dot{y}(t) &= \underbrace{\nabla_x h(x(t))}_{C_c(x(t),u(t))} \dot{x}(t).\end{aligned} \tag{9}$$

The subscript 'c' indicates *continuous-time*. An important remark is that the steady-state information is lost during the process of differentiation when using velocity-based linearization [17]. Nevertheless, the steady-state information on the output can be recovered by state augmentation:

$$\begin{aligned}\underbrace{\begin{bmatrix}\dot{y}(t)\\ \ddot{x}(t)\end{bmatrix}}_{\dot{x}_{ext}(t)} &= \underbrace{\begin{bmatrix}0 & C_c(x(t),u(t))\\ 0 & A_c(x(t),u(t))\end{bmatrix}}_{A_{c,ext}(x(t),u(t))} \underbrace{\begin{bmatrix}y(t)\\ \dot{x}(t)\end{bmatrix}}_{x_{ext}(t)} + \underbrace{\begin{bmatrix}0\\ B_c(x(t),u(t))\end{bmatrix}}_{B_{c,ext}(x(t),u(t))} \dot{u}(t),\\ y(t) &= \underbrace{\begin{bmatrix}I & 0\end{bmatrix}}_{C_{c,ext}} \underbrace{\begin{bmatrix}y(t)\\ \dot{x}(t)\end{bmatrix}}_{x_{ext}(t)}.\end{aligned} \tag{10}$$

This can be written as a quasi-LPV model by setting $\theta = H[x(t)^\top, u(t)^\top]^\top \in \mathbb{R}^{n_\theta}$, where H is a selector matrix.[2] Discretizing (10) gives:

$$\begin{aligned}x_{k+1,ext} &= A_{d,ext}(\theta_k) x_{k,ext} + B_{d,ext}(\theta_k) \Delta u_k,\\ y_k &= C_{d,ext} x_{k,ext},\end{aligned} \tag{11}$$

with $x_{k,ext} = [y_k^\top \quad \Delta x_k^\top,]^\top$, $\Delta u_k = u_k - u_{k-1}$, and the subscript 'd' stands for *discrete-time*. The discretized model can be obtained through a variety of well-known methods [21].

D. Velocity-Based qLMPC Algorithm

This section combines the established theory of the conventional qLMPC algorithm with velocity-based linearization to create a velocity-based qLMPC algorithm.

When working in velocity space, all equilibrium or operating points are mapped to the origin. This characteristic makes the velocity-based qLMPC framework parameterization-free, as there is no need to calculate steady-state values for the state vector and input. This contrasts with the technique used, for example, in [11]. Moreover, stability can be guaranteed without the need for complex offline computations. First, the optimization problem formulation for the velocity-based qLMPC is provided:

$$\begin{aligned}&\min_{\Delta u} \; J_k(\Delta u)\\ &\text{s.t.} \quad \begin{bmatrix}y_{k+i}\\ \Delta x_{k+i}\end{bmatrix} = A_d(\theta_{k+i-1}) \begin{bmatrix}y_{k+i-1}\\ \Delta x_{k+i-1}\end{bmatrix} + B_d(\theta_{k+i-1}) \Delta u_{k+i-1},\\ &\qquad u_{k+i-1} = u_{k-1} + \sum_{j=1}^{i} \Delta u_{k+j-1} \in \mathcal{U},\\ &\qquad x_{k+i-1} \in \mathcal{X} \quad \forall i \in [1, \ldots, N], \quad \Delta x_{k+N} = 0,\end{aligned} \tag{12}$$

with the cost function being defined as

$$\begin{aligned}J_k(\Delta u) = \sum_{i=1}^{N} \Big(&||y_{k+i-1} - y_{ref}||_{Q_1}^2 + ||\Delta x_{k+i-1}||_{Q_2}^2\\ &+ ||\Delta u_{k+i-1}||_R^2 \Big) + ||y_{k+N} - y_{ref}||_P^2,\end{aligned} \tag{13}$$

Note that the cost function in (13) includes a penalization on the extended state vector x_{ext} with the weighting matrix $Q_1 \in \mathbb{R}^{n_y \times n_y}$ acting on y and $Q_2 \in \mathbb{R}^{n_{\Delta x} \times n_{\Delta x}}$ on Δx. There is also a penalty for the control input Δu given by the weighting matrix $R \in \mathbb{R}^{n_{\Delta u} \times n_{\Delta u}}$, and a terminal cost that penalizes reference deviations at the end of the horizon.

In (12), the constraint defined as $\Delta x_{k+N} = 0$ guarantees that the state corresponding to y_{k+N} is a steady state. With this, the recursive feasibility of the optimization problem can be achieved for a set of feasible initial conditions, which is a necessary condition for stability. Also, the cost function is a decaying sequence, $J_{k+1} \leq J_k$, due to the terminal cost, and thus the closed-loop is stable. For the complete proof, please refer to [22].

Having these concepts, the following section gives insights into the MDT technique mentioned earlier in this letter.

IV. Model Demodulation Transformation

This section provides the main results for the MDT technique which is used in this letter to provide the frequency-dependent dynamical behavior as a steady-state signal. For a more detailed derivation, the reader is referred to [23].

Let a periodic signal $x_i(t)$ be represented as:

$$x_i(t) = a_i(\tau) \cos(\omega_r t + \phi(\tau)). \tag{14}$$

Given that the amplitude a_i and phase ϕ exhibit a slower rate of change, a new time coordinate is introduced, denoted as τ. A function $f(\tau)$ is considered slow when compared to a rapidly varying periodic function $g(t)$ with period T if the following property holds [23]:

$$\int_0^T f(\tau) g(t) \mathrm{d}t \approx f(\tau) \int_0^T g(t) \mathrm{d}t. \tag{15}$$

The periodic signal can be re-written using Euler's formula:

$$x_i(t) = \Re\{\underbrace{a_i(\tau) e^{j\phi(\tau)}}_{X_i(\tau)} e^{j\omega_r t}\}, \tag{16}$$

with $X_i(\tau) \in \mathbb{C}$ being a slow-varying function. Taking the first-time derivative gives:

$$\dot{x}_i(t) = \Re\Big\{\big(\dot{X}_i(\tau) + j\omega_r X_i(\tau)\big) e^{j\omega_r t}\Big\}. \tag{17}$$

The amplitude and phase of the original periodic signal in (14) can be reconstructed using the following relations:

$$a_i(\tau) = ||\Re\{X_i(\tau)\}, \Im\{X_i(\tau)\}||_2, \quad \phi_i(\tau) = \operatorname{atan}\Big(\frac{\Im\{X_i(\tau)\}}{\Re\{X_i(\tau)\}}\Big).$$

[2] A selector matrix is characterized by having one entry of 1 per row, at most one entry of 1 per column, and all other entries 0 [20].

Having these insights into the MDT technique, the following section provides the steps to obtain the wind turbine aerodynamics and tower demodulated model.

V. Application in Wind Turbine Control

The MDT technique previously introduced is used here to demodulate the tower dynamics and also augment the model with a wind turbine aerodynamic model to enable self-scheduling via the quasi-LPV model structure. The resulting model is then linearized using velocity-based linearization and controlled with a velocity-based qLMPC. Hence, the proposed framework combines approaches from [11] and [13].

A. Nominal Model

The nominal tower dynamics are given as the following spring-mass-damper second-order linear model [24], [25]:

$$\begin{bmatrix}\dot{x}_1(t)\\ \dot{x}_2(t)\end{bmatrix}=\begin{bmatrix}-\frac{d}{m} & -\frac{k}{m}\\ 1 & 0\end{bmatrix}\begin{bmatrix}x_1(t)\\ x_2(t)\end{bmatrix}+\begin{bmatrix}\frac{1}{m}\\ 0\end{bmatrix}\big(F_{\mathrm{sd}}+c\Delta T_{\mathrm{g}}+cT_{\mathrm{g}}\big), \tag{18}$$

with $\{m, d, k\} \in \mathbb{R}^+$ being the constant modal mass, modal damping, and modal stiffness. The tower dynamics are affected by the generator torques T_{g} and ΔT_{g}, which are considered as the control actions in this letter. The torque T_{g} is used mainly in power production, while the additive torque ΔT_{g} is used to mitigate the side-side periodic load F_{sd}. The constant $c = 3/2H$ defines the ratio between the angular and translational displacement of the tower motion under the assumption that the tower is a prismatic beam [26] and H is the tower height. The states $x_1(t)$ and $x_2(t)$ represent the tower's top velocity and displacement, respectively, in the side-side direction. Here, F_{sd} and ΔT_{g} are modeled as:

$$F_{\mathrm{sd}} = a_{\mathrm{sd}}(\tau)\cos(\psi(t)), \quad \Delta T_{\mathrm{g}} = a_{\mathrm{g}}(\tau)\cos\big(\psi(t)+\phi_{\mathrm{g}}(\tau)\big),$$

with $a_{\mathrm{sd}}(\tau) \in \mathbb{R}^+$ being the amplitude of the excitation, $a_{\mathrm{g}}(\tau) \in \mathbb{R}^+$ the amplitude of the control signal, $\psi(t) \in [0, 2\pi)$ the rotor azimuth angle, and $\phi_{\mathrm{g}}(\tau) \in [0, 2\pi)$ the phase of the control signal. Also relevant is the representation of the complete wind turbine aerodynamics:

$$\dot{\omega}_{\mathrm{r}} = \frac{T_{\mathrm{a}}-G(T_{\mathrm{g}}+\Delta T_{\mathrm{g}})}{J_{\mathrm{r}}}, \quad T_{\mathrm{a}} = \tfrac{1}{2}\rho\pi R^3 V^2 C_{\mathrm{q}}(\lambda,\beta), \quad T_{\mathrm{g}} = \tfrac{K}{G}\omega_{\mathrm{r}}^2,$$

with $T_{\mathrm{a}} \in \mathbb{R}$ being the aerodynamic rotor torque, $G \geq 1$ the gearbox ratio, and $J_{\mathrm{r}} \in \mathbb{R}^+$ the total rotor inertia. The optimal mode gain K is defined as $K = \pi\rho R^5 C_{\mathrm{p}}(\lambda^\star, \beta^\star)/2\lambda^{\star^3} \in \mathbb{R}^+$. Furthermore, $\rho \in \mathbb{R}^+$ is the air density, $R \in \mathbb{R}^+$ the rotor radius, $V \in \mathbb{R}^+$ the wind speed, $\omega_{\mathrm{r}} \in \mathbb{R}^+$ the rotor speed, $C_{\mathrm{q}} \in \mathbb{R}^+$ the aerodynamic torque coefficient, and $C_{\mathrm{p}} \in \mathbb{R}^+$ the power coefficient as a function of the designed tip-speed ratio $\lambda^\star = \omega_{\mathrm{r}}^\star R/V$ and the fine pitch angle $\beta^\star$.

B. Demodulated Model

Assuming a constant rotor's angular velocity over one revolution $T_{\mathrm{r}} = 2\pi/\omega_{\mathrm{r}}$, the following holds:

$$\psi(t) = \int \omega_{\mathrm{r}}\mathrm{d}t \approx \omega_{\mathrm{r}} t, \tag{19}$$

The side-side periodic load and the (total) generator torque signals can be decomposed into their semi-harmonic components and re-written as follows [12]:

$$F_{\mathrm{sd}} + c\Delta T_{\mathrm{g}} + cT_{\mathrm{g}} = \Re\left\{a_{\mathrm{sd}}(\tau)e^{\mathrm{j}\omega_{\mathrm{r}}t} + ca_{\mathrm{g}}(\tau)e^{\mathrm{j}\phi_{\mathrm{g}}(\tau)}e^{\mathrm{j}\omega_{\mathrm{r}}t} + c\sum_{n=0}^{\infty}\mathrm{T}_{\mathrm{g}}^{(n)}(\tau)e^{\mathrm{j}n\omega_{\mathrm{r}}t}\right\}, \tag{20}$$

Applying (16), (17) and (20) to the state-space in (18) and multiplying by $e^{\mathrm{j}\omega_{\mathrm{r}}t}$ followed by integration over an oscillation period gives:

$$\int_0^{T_r}\Re\left\{\Big(\dot{X}_1(\tau)+\mathrm{j}\omega_{\mathrm{r}}X_1(\tau)+\tfrac{d}{m}X_1(\tau)+\tfrac{k}{m}X_2(\tau)-\tfrac{1}{m}a_{\mathrm{sd}}(\tau) - \tfrac{c}{m}a_{\mathrm{g}}(\tau)e^{\mathrm{j}\phi_{\mathrm{g}}(\tau)}\Big)e^{\mathrm{j}\omega_{\mathrm{r}}t} - \tfrac{c}{m}\sum_{n=0}^{\infty}\mathrm{T}_{\mathrm{g}}^{(n)}(\tau)e^{\mathrm{j}n\omega_{\mathrm{r}}t}\right\}e^{\mathrm{j}\omega_{\mathrm{r}}t}\mathrm{d}t = 0,$$

$$\int_0^{T_r}\Re\Big\{\big(\dot{X}_2(\tau)+\mathrm{j}\omega_{\mathrm{r}}X_2(\tau)-X_1(\tau)\big)e^{\mathrm{j}\omega_{\mathrm{r}}t}\Big\}e^{\mathrm{j}\omega_{\mathrm{r}}t}\mathrm{d}t = 0.$$

Note that the τ notation is dropped for the remainder of this letter for brevity. Applying the result from (15) leads to:

$$\begin{bmatrix}\dot{X}_1\\ \dot{X}_2\end{bmatrix}=\begin{bmatrix}-\mathrm{j}\omega_{\mathrm{r}}-\frac{d}{m} & -\frac{k}{m}\\ 1 & -\mathrm{j}\omega_{\mathrm{r}}\end{bmatrix}\begin{bmatrix}X_1\\ X_2\end{bmatrix}+\begin{bmatrix}\frac{c}{m}\\ 0\end{bmatrix}\underbrace{a_{\mathrm{g}}e^{\mathrm{j}\phi_{\mathrm{g}}}}_{A_{\mathrm{g}}}+\begin{bmatrix}\frac{1}{m}\\ 0\end{bmatrix}a_{\mathrm{sd}}.$$

In the above equation, the 1P contribution of T_{g} in the tower dynamics, i.e., $\mathrm{T}_{\mathrm{g}}^{(1)}$, is neglected (c.f. [12]) as it is minor compared to the 1P disturbance from rotor imbalance.

Setting $[q_1, q_2, q_3, q_4]^\top = [\Re\{X_1\}, \Im\{X_1\}, \Re\{X_2\}, \Im\{X_2\}]^\top$, and adding the representation of the complete aerodynamics, the system can be defined as the following:

$$\begin{aligned}
\dot{q}_1 &= f_1 = -\tfrac{d}{m}q_1 + \omega_{\mathrm{r}}q_2 - \tfrac{k}{m}q_3 + \tfrac{c}{m}\Re\{A_{\mathrm{g}}\} + \tfrac{a_{\mathrm{sd}}}{m},\\
\dot{q}_2 &= f_2 = -\omega_{\mathrm{r}}q_1 - \tfrac{d}{m}q_2 - \tfrac{k}{m}q_4 + \tfrac{c}{m}\Im\{A_{\mathrm{g}}\},\\
\dot{q}_3 &= f_3 = q_1 + \omega_{\mathrm{r}}q_4, \quad \dot{q}_4 = f_4 = q_2 - \omega_{\mathrm{r}}q_3,\\
\dot{\omega}_{\mathrm{r}} &= f_5 = \tfrac{T_{\mathrm{a}}-G(T_{\mathrm{g}}+\Delta T_{\mathrm{g}})}{J_{\mathrm{r}}},
\end{aligned} \tag{21}$$

where

$$\Delta T_{\mathrm{g}} = ||\Re\{A_{\mathrm{g}}\}, \Im\{A_{\mathrm{g}}\}||_2 \cos\Big(\omega_{\mathrm{r}}t + \mathrm{atan}\Big(\tfrac{\Im\{A_{\mathrm{g}}\}}{\Re\{A_{\mathrm{g}}\}}\Big)\Big)$$

is the previously mentioned periodic torque signal set as the control input to mitigate the side-side load.

C. Velocity-Based qLMPC for Side-Side Periodic Load Mitigation

This subsection mathematically formalizes the velocity-based qLMPC used for side-side periodic load mitigation. First, the model presented in (21) is linearized using the velocity-based linearization technique described in (9). Hence, by defining:

$$\begin{aligned}
x &= \begin{bmatrix}q_1 & q_2 & q_3 & q_4 & \omega_{\mathrm{r}} & V & a_{\mathrm{sd}}\end{bmatrix}^\top \in \mathbb{R}^{7\times 1},\\
u &= \begin{bmatrix}\Re\{A_{\mathrm{g}}\} & \Im\{A_{\mathrm{g}}\}\end{bmatrix}^\top \in \mathbb{R}^{2\times 1}, \quad y = \begin{bmatrix}q_1 & q_2 & q_3 & q_4 & \omega_{\mathrm{r}}\end{bmatrix}^\top \in \mathbb{R}^{5\times 1},
\end{aligned} \tag{22}$$

the following can be derived:

$$\ddot{x} = \underbrace{\begin{bmatrix}
-\frac{d}{m} & \omega_{\mathrm{r}} & -\frac{k}{m} & 0 & q_2 & 0 & \frac{1}{m}\\
-\omega_{\mathrm{r}} & -\frac{d}{m} & 0 & -\frac{k}{m} & -q_1 & 0 & 0\\
1 & 0 & 0 & \omega_{\mathrm{r}} & q_4 & 0 & 0\\
0 & 1 & -\omega_{\mathrm{r}} & 0 & -q_3 & 0 & 0\\
0 & 0 & 0 & 0 & \frac{\partial\dot{\omega}_{\mathrm{r}}}{\partial\omega_{\mathrm{r}}} & \frac{\partial\dot{\omega}_{\mathrm{r}}}{\partial V} & 0\\
0 & 0 & 0 & 0 & 0 & 0 & 0\\
0 & 0 & 0 & 0 & 0 & 0 & 0
\end{bmatrix}}_{A_{\mathrm{c}}(x,u)}\dot{x}$$

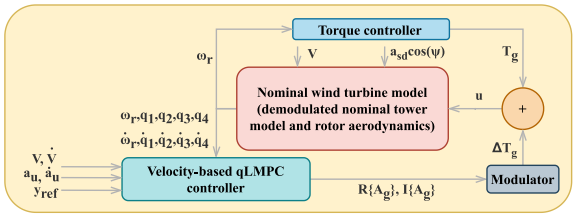

Fig. 1. Block diagram of the closed-loop control scheme used in the simulation case. The nonlinear wind turbine model includes the demodulated nominal tower model, rotor aerodynamics, and the generator torque and velocity-based qLMPC controllers.

$$+\underbrace{\begin{bmatrix} \frac{c}{m} & 0 \\ 0 & \frac{c}{m} \\ 0 & 0 \\ 0 & 0 \\ \frac{\partial\dot{\omega}_r}{\partial\Re\{A_g\}} & \frac{\partial\dot{\omega}_r}{\partial\Im\{A_g\}} \\ 0 & 0 \\ 0 & 0 \end{bmatrix}}_{B_c(x,u)} \dot{u},$$

$$\dot{y} = \underbrace{\begin{bmatrix} I_{5\times5} & 0_{5\times2} \end{bmatrix}}_{C_c} \dot{x},$$

with

$$\begin{aligned} \frac{\partial\dot{\omega}_r}{\partial\omega_r} &= \frac{\rho\pi R^4}{2J_r}\frac{\partial C_q(\lambda,\beta)}{\partial\lambda}V - \frac{2K}{J_r}\omega_r, \\ \frac{\partial\dot{\omega}_r}{\partial V} &= \frac{\rho\pi R^3 C_q(\lambda,\beta)}{J_r}V - \frac{\rho\pi R^4}{2J_r}\frac{\partial C_q(\lambda,\beta)}{\partial\lambda}\omega_r, \\ \frac{\partial\dot{\omega}_r}{\partial\Re\{A_g\}} &= -\frac{G}{J_r}\cos(\omega_r t), \quad \frac{\partial\dot{\omega}_r}{\partial\Im\{A_g\}} = -\frac{G}{J_r}\sin(\omega_r t), \end{aligned} \tag{23}$$

and where $A_c(x,u) \in \mathbb{R}^{7\times7}$ and $B_c(x,u) \in \mathbb{R}^{7\times2}$ are the state and input matrices, respectively, and $C_c \in \mathbb{R}^{5\times7}$ is the output matrix. Note that in the partial derivative of $\dot{\omega}_r$ with respect to ω_r, the terms corresponding to the influence of the control action are zero due to the assumption of a constant rotor's angular velocity over one revolution in (19).

Now a velocity-form state-dependent linear model is defined in continuous time as in (10). Note that here the output $y \in \mathbb{R}^{5\times1}$ is chosen to be $\{q_1, q_2, q_3, q_4, \omega_r\}$. Also, the state and input matrices depend on those parameters and the wind speed. Therefore, this can be written as a quasi-LPV model by setting $\theta = [q_1 \quad q_2 \quad q_3 \quad q_4 \quad \omega_r \quad V]^\top \in \mathbb{R}^{6\times1}$. The continuous state-space is then discretized with sampling time t_s using the forward Euler method. The discrete-time wind turbine model is described as in (11).

The optimization problem outlined earlier in equation (12) aims to minimize the cost specified in equation (13) and is applied to the model derived in this section. It can be deduced that, taking into account the whole prediction horizon, $||\mathbf{y} - \mathbf{y}_{ref}||^2_{Q_1}$ aims to minimize periodic fatigue loads, whereas $||\Delta\mathbf{u}||^2_R$ is a combination of impact on energy production minimization and penalization on the control input. With this cost function, a trade-off is possible between the influence in power production and load reductions.

VI. Simulation Case

This section presents simulation results using a nonlinear aerodynamic wind turbine model to assess the performance of the proposed framework.[3] Fig. 1 depicts the simulation setup.

[3]The MATLAB Simulink implementation is made available in [28].

TABLE I
Parameters of the (Modified) NREL 5-MW Reference Wind Turbine in the Partial-Load Operating Region [5], [27]

Parameter	Symbol	Value	Units
Gearbox ratio	G	97	-
LSS equivalent inertia	J_r	4.0802×10^7	kg m^2
Rotor radius	R	63	m
Tower height	H	90	m
Tower modal mass	m	3.6200×10^5	kg
Tower modal damping	d	2.4588×10^3	kg s^{-1}
Tower modal stiffness	k	1.7677×10^5	kg s^{-2}
Tower natural frequency	ω_n	0.7071	rad s^{-1}

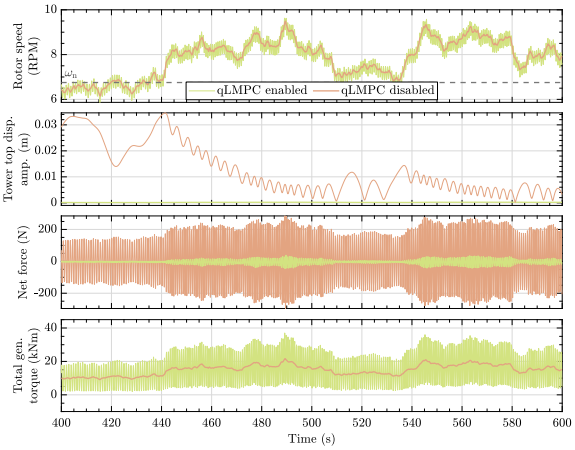

Fig. 2. Rotor speed, tower top displacement amplitude, net force applied to the tower, and total generator torque when the velocity-based qLMPC controller is disabled and when it is enabled. The designed controller significantly influences the rotor speed by superimposing a periodic signal. However, it effectively reduces the net force, considerably diminishing the tower top displacement amplitude.

According to **Assumptions** 2 and 3, the states, wind, and disturbance are known; however, in realistic conditions these should be estimated [12].

The parameters of the (modified) NREL 5-MW reference wind turbine in the partial-load operating region can be found in Table I. Originally, the tower of this reference turbine was classified as soft-stiff but here altered into soft-soft by adjusting the modal parameters, representing wall thickness reductions. The controller parameters are defined as follows: $t_s = 0.1$ s, $N = 25$, $Q_1 = \text{diag}(1, 1, 5, 5, 0) \times 10^3$, $Q_2 = \text{diag}(1, 1, 1, 1, 0, 0, 0) \times 10^3$, $R = \text{diag}(1, 1) \times 10^{-8}$, and $P = 2Q_1$. Hence, the prediction horizon is set to 2.5 s. The side-side periodic load amplitude is driven by a rotor-speed-dependent centrifugal force $a_{sd} = mr\omega_r^2$, where $mr = 300$ kg m models a 0.06% imbalance of one blade with respect to two other blades. To evaluate the performance of the designed algorithm, the model is subjected to a realistic turbulent case with a mean wind speed at hub height of 6.5 m/s and turbulence intensity of 20% for 600 s. Turbulence intensity determines the standard deviation of the longitudinal wind speed given a hub-height wind speed as detailed in [29]. In one simulation, the controller remains disabled for the entirety of the simulation time, whereas, in the other, the controller is enabled from the start. The side-side periodic load is applied at $t = 10$ s. As the controller aims for complete attenuation of the side-side load, the tower top displacement reference is set to zero ($\mathbf{y}_{ref} = 0$).

Results of this turbulent case are presented in Fig. 2, shown for $t = 400 - 600$ s. The uncontrolled wind turbine signals

are shown by the orange lines and those with the designed velocity-based qLMPC controller are shown by the green lines. It can be noticed that the velocity-based qLMPC controller considerably influences the rotational speed by superimposing a periodic torque signal. Nevertheless, the controller shows its efficiency in reducing the effects of the side-side periodic load by bringing the net force down by 96% on average, in effect leading to significant tower top displacement reductions. This is particularly relevant when the rotor speed acts around the tower's resonance frequency. However, it is important to realize that these results show the maximum potential of the developed control scheme; in practical scenarios, a trade-off needs to be made for load attenuation and actuation. Additionally, the velocity-based qLMPC algorithm converges to the optimal scheduling sequence in a maximum of two iterations, taking an average of 0.02 s to solve the optimal control problem per time step.

VII. Conclusion

This letter introduces a novel approach to wind turbine tower load control, focusing on mitigating side-side periodic loads through a velocity-based qLMPC framework. By employing strategic coordinate transformations, such as MDT and velocity-based linearization, the method enhances wind turbine control strategies and effectively reduces load impacts. A simulation in realistic turbulent wind conditions validates the algorithm's effectiveness and practicality. While the proposed control algorithm may require more complex tuning compared to traditional solutions, its performance and computational benefits make it a valuable alternative.

Due to the high influence of the control action's periodicity on the rotor speed, this method also highly influences power production as there is a direct relation with the (total) generator torque, considered as the control input here. Future work may focus on changing the optimization problem to partially reduce the tower-top displacement in a trade-off with actuation effort, rather than complete attenuation of the periodic load as in this letter.

References

[1] (Intergovt. Panel Climate Change, Geneva, Switzerland). *Renewable Energy Sources and Climate Change Mitigation—IPCC*. May 2024. [Online]. Available: https://www.ipcc.ch/report/renewable-energy-sources-and-climate-change-mitigation

[2] K. Dykes, R. Damiani, O. Roberts, and E. Lantz, "Analysis of ideal towers for tall wind applications," in *Proc. Wind Energy Symp.*, Jan. 2018, pp. 1–11.

[3] J. Niebsch and R. Ramlau, "Simultaneous estimation of mass and aerodynamic rotor imbalances for wind turbines," *J. Math. Ind.*, vol. 4, p. 12, Sep. 2014.

[4] Z. Zhang, S. R. K. Nielsen, F. Blaabjerg, and D. Zhou, "Dynamics and control of lateral tower vibrations in offshore wind turbines by means of active generator torque," *Energies*, vol. 7, no. 11, pp. 7746–7772, Nov. 2014.

[5] A. K. Pamososuryo, S. P. Mulders, R. Ferrari, and J.-W. van Wingerden, "On the analysis and synthesis of wind turbine side–side tower load control via demodulation," *IEEE Trans. Control Syst. Technol.*, vol. 32, no. 5, pp. 1865–1880, Sep. 2024.

[6] D. Duckwitz and M. Geyler, "Active damping of the side-to-side oscillation of the tower," in *Proc. DEWEK*, 2010, pp. 1–4.

[7] A. K. Pamososuryo, Y. Liu, T. G. Hovgaard, R. Ferrari, and J. W. van Wingerden, "Individual pitch control by convex economic model predictive control for wind turbine side-side tower load alleviation," *J. Phys., Conf. Ser.*, vol. 2265, May 2022, Art. no. 32071.

[8] B. Fischer and M. Shan, "A survey on control methods for the mitigation of tower loads," Fraunhofer-Inst. Wind Energy Syst. Technol., Bremerhaven, Germany, Rep. 01/104256, 2013.

[9] P. Schaak, G. Corten, and E. Van der Hooft, "Crossing resonance rotor speeds of wind turbines," Energy Res. Centre The Netherlands, Petten, The Netherlands, Rep. ECN-RX-03-041, 2003.

[10] J. Licari, J. B. Ekanayake, and N. Jenkins, "Investigation of a speed exclusion zone to prevent tower resonance in variable-speed wind turbines," *IEEE Trans. Sustain. Energy*, vol. 4, no. 4, pp. 977–984, Oct. 2013.

[11] S. P. Mulders, T. G. Hovgaard, J. D. Grunnet, and J. W. van Wingerden, "Preventing wind turbine tower natural frequency excitation with a quasi-LPV model predictive control scheme," *Wind Energy*, vol. 23, no. 3, pp. 627–644, Mar. 2020.

[12] A. K. Pamososuryo, S. P. Mulders, R. Ferrari, and J.-W. van Wingerden, "Periodic load estimation of a wind turbine tower using a model demodulation transformation," in *Proc. ACC*, 2022, pp. 8–10.

[13] A. Dittmer, B. Sharan, and H. Werner, "A velocity quasiLPV-MPC algorithm for wind turbine control," in *Proc. ECC*, Jun. 2021, pp. 1550–1555.

[14] E. F. Camacho and C. Bordons, "Nonlinear model predictive control: An introductory review," in *Assessment and Future Directions of Nonlinear Model Predictive Control*, R. Findeisen, F. Allgöwer, and L. T. Biegler, Eds., Berlin, Germany: Springer, 2007, pp. 1–16, doi: 10.1007/978-3-540-72699-9_1.

[15] J. S. Shamma and M. Athans, "Analysis of gain scheduled control for nonlinear plants," *IEEE Trans. Autom. Control*, vol. 35, no. 8, pp. 898–907, Aug. 1990.

[16] J. Mohammadpour and C. W. Scherer, *Control of Linear Parameter Varying Systems with Applications*. New York, NY, USA: Springer, 2012.

[17] G. Cisneros and P. Sebastian, "Quasi-linear model predictive control: Stability, Modelling and implementation," Ph.D. dissertation, Inst. Control Syst., Technische Universität Hamburg, Hamburg, Germany, 2021.

[18] W. J. Rugh and J. S. Shamma, "Research on gain scheduling," *Automatica*, vol. 36, no. 10, pp. 1401–1425, 2000. [Online]. Available: https://www.sciencedirect.com/science/article/pii/S0005109800000583

[19] P. S. G. Cisneros, S. Voss, and H. Werner, "Efficient nonlinear model predictive control via quasi-LPV representation," in *Proc. IEEE CDC*, 2016, pp. 3216–3221.

[20] R. Toth, H. S. Abbas, and H. Werner, "On the state-space Realization of LPV input-output models: Practical approaches," *IEEE Trans. Control Syst. Technol.*, vol. 20, no. 1, pp. 139–153, Jan. 2012.

[21] D. Griffiths and D. J. Higham, *Numerical Methods for Ordinary Differential Equations: Initial Value Problems* (Springer Undergraduate Mathematics Series). London, U.K.: Springer, 2010. [Online]. Available: https://books.google.nl/books?id=HrrZop_3bacC

[22] P. S. G. Cisneros and H. Werner, "A velocity algorithm for nonlinear model predictive control," *IEEE Trans. Control Syst. Technol.*, vol. 29, no. 3, pp. 1310–1315, May 2021.

[23] A. K. Janbahan, M. S. Tamer, J. W. van Wingerden, J. F. L. Goosen, and A. van Keulen, "A comprehensive model for transient behavior of tapping mode atomic force microscope," *Nonlin. Dyn.*, vol. 97, no. 2, pp. 1601–1617, 2019.

[24] E. A. Bossanyi, "The design of closed loop controllers for wind turbines," *Wind Energy*, vol. 3, no. 3, pp. 149–163, Jul. 2000.

[25] M. A. Evans, M. Cannon, and B. Kouvaritakis, "Robust MPC tower damping for variable speed wind turbines," *IEEE Trans. Control Syst. Technol.*, vol. 23, no. 1, pp. 290–296, Jan. 2015.

[26] K. Selvam, S. Kanev, J. W. van Wingerden, T. van Engelen, and M. Verhaegen, "Feedback–feedforward individual pitch control for wind turbine load reduction," *Int. J. Robust Nonlin. Control*, vol. 19, no. 1, pp. 72–91, Jan. 2009.

[27] J. Jonkman, S. Butterfield, W. Musial, and G. Scott, "Definition of a 5-MW reference wind turbine for offshore system development," Nat. Renew. Energy Lab., Golden, CO, USA, Rep. NREL/TP-500-38060, Feb. 2009.

[28] M. de Fonseca, A. K. Pamososuryo, and S. P. Mulders (Zenodo, Genève, Switzerland). *Software Implementation: Efficient Velocity-Based Quasi-Linear Model Predictive Control for Wind Turbine Side-Side Tower Periodic Load Reductions*. 2024. [Online]. Available: https://doi.org/10.5281/zenodo.14004355

[29] *Wind Turbines—Part-1: Design Requirements*, IEC Standard 61400-1, Aug. 2005.